Growth of ultrathin silicon nitride on Si(111) at low temperatures

A. Bahari, U. Robenhagen, and P. Morgen

Fysisk Institut, University of Southern Denmark, Odense, Denmark

Z. S. Li

ISA, Department of Physics and Astronomy, University of Aarhus, Aarhus, Denmark

Nitrogen mixed into silicon dioxide on Si(100) is used in the present, and maybe last, generation of silicon oxide-based complementary metal-oxide semiconductor (CMOS) components to improve various properties of the gate dielectric. A pure nitride layer could offer certain advantages, but has been found to be less optimal than oxide for Si(100). In this work, the growth of pure ultrathin (<3 nm) silicon nitride films directly on Si(111) is achieved in reactions between the Si surface and atomic N, in an isothermal process at low temperatures (300 °C to 800 °C) using a remote, microwave-excited nitrogen plasma connected to an ultrahigh vacuum chamber through a pressure differential stage. For this system, recent results have shown the possibility of a good interface with epitaxial crystalline Si_3N_4. In the present work, attention is paid to understanding the conditions separating the growth of amorphous ultrathin silicon nitride from the growth of crystalline structures during this process because the amorphous, ultrathin silicon nitride might be the best substitute for silicon oxide since ultrathin crystalline films grown in this way are microcrystalline.

PACS number(s): 81.15.−z, 82.45.Mp, 79.60.Dp

I. INTRODUCTION

Two issues are seriously discussed as threats to the use of ultrathin (<1–2 nm) pure oxides of silicon in the next complementary metal-oxide semiconductor (CMOS) device generations. One is oxide degradation due to boron penetration from the poly-silicon gate electrode, and the other is electron tunneling through the oxide.[1,2] The approach to avoid boron diffusion is to use a tailored and spatially controlled nitrogen incorporation into the silicon oxide or silicon-oxy-nitrides. Many potential high-K gate dielectrics have been studied because they obtain the desired EOT (effective oxide thickness referred to pure SiO_2) as a physically much thicker film, thus avoiding the problems of tunneling. They have been intensively studied but without definitive success, due to degradation of the channel mobility from metal out-diffusion and reactions with silicon at the interface and in the channel region. However, pure, hydrogen-free ultrathin Si_3N_4 should be more intensively studied as a higher-K gate dielectric material with potential for the next device generations.[3,4]

The growth procedures and properties of ultrathin films are challenging, compared to thicker films, and appropriate methods to follow the growth and to detect the structure of the interface and the bulk of the film are important. For this we use photoemission with high resolution, with an electron storage ring as the light source.

Nitrogen incorporation in gate oxides, in previous and current CMOS generations, is carried out with furnace processing,[5] RTP (rapid thermal processing),[6] or in a downstream plasma process.[7] These procedures have been done with different nitrogen-containing gases. However, the use of atomic N instead of NO,[8,9] N_2O,[7,10,11] or NH_3,[12,13] was shown to reduce an adverse influence on peak carrier mobility in the channel of metal-oxide-semiconductor field-effect transistors (MOSFETs). It also serves to reduce hot electron-induced degradation,[14] and it avoids hydrogen and oxygen content in the films.[15,16] The process of nitridation[17–19] using NH_3 introduces electron traps in the nitride film due to the unavoidable incorporation of H, thus plasma-assisted nitridation is currently one of the most promising methods to form hydrogen-free nitrided gate dielectric films, and the gas excitation lowers the necessary reaction temperature.

Crystalline Si_3N_4 is a wide band-gap (5.3 eV) material.[20] The interface between crystalline Si_3N_4 and Si(100) is significantly more stable and impenetrable than for any other high-K dielectric.[21] The permittivity of Si_3N_4 is about eight, or twice that of SiO_2. As a disadvantage, Ref. 22, however, claims that unsatisfied bonds are unavoidable in bulk silicon nitride. The interfacial strain is lower for this system, compared to SiO_2 on Si(100), and because of free-energy terms, the interface is thermodynamically stable. Nitrogen atoms in the bulk of the nitride, or at the interface, will compete favorably with boron for occupation of defect sites in the bulk.

A recent study[18] has shown that ammonia-based thermal nitridation reactions in ultra high vacuum (UHV) are self limiting at very low thicknesses in the same range of temperatures used here for isothermal growth. That study also demonstrated how ultrathin Si_3N_4 layers may be used as diffusion barriers below the high-K dielectric film, although some carrier mobility degradation in the channel was still noticeable. The self-limiting nitride thickness was found to increase with increasing temperature.

We have performed a series of studies of the Si(111), and later the Si(100) surface, and the gradual growth of Si_3N_4 on top, from the reaction with N (from plasma excited nitrogen gas), at 300 °C and for a range of temperatures up to 800 °C. These studies were performed using synchrotron radiation-induced photoelectron spectroscopy and conventional x-ray photoemission spectroscopy (XPS). Using these techniques, we can study the chemical bonding configuration

at the surface and at the interface of Si_3N_4 and the Si surfaces, the composition and structure in the bulk of the nitride layer, and we can estimate the film thickness. The Si(111) surface was chosen initially because it offers more spectroscopical details of the reaction, showing more clearly how the interface behaves, while it could be argued that the Si(100) surface has more appeal due to its use in all current CMOS device fabrication. However, our results show that the interface structure on Si(100) is more complex than for Si(111), and probably prohibitive to its use in devices. These studies have been completed recently and will be published separately.

II. EXPERIMENTAL DETAILS AND RESULTS

The samples, (Si(111) *n*-type, 5 Ω cm, 3 cm×1 cm), were cut out of 1 mm thick wafers, mounted in a holder, and introduced in the UHV chamber after a rinse of the sample and holder with ethanol in an ultrasonic bath. All further cleaning was done inside the UHV chamber by heating the sample by passing a direct current through it, initially to 1100 °C. Later, after growing various thicknesses of nitride films on the surface, higher temperatures were needed to restore a clean Si surface. Nitrogen gas was leaked into a discharge tube connected to the UHV system through a capillary, and the 2.5 GHz microwave radiation-excited plasma of nitrogen was sent into the reaction chamber through this capillary, acting as a differential between the pressure in the excitation region and the UHV. The background pressure in the UHV chamber during spectroscopic measurements was of the order of 10^{-10} Torr.

Measurements with a quadrupole mass spectrometer show that a very high proportion of atomic N ($>50\%$) typically exists inside the UHV chamber with this setup. The typical total nitrogen pressure in the chamber during nitrogen exposure was 2×10^{-7} Torr. The Si(111) substrate is kept at a temperature of 300 °C or above. Temperatures (above 400 °C) are measured by an optical pyrometer.

The signs of the beginning nitridation are evident from the spectra shown in Figs. 1 and 2. These figures show the results of adsorbing nitrogen on a moderately heated Si(111) surface, on the Si $2p$ high-resolution core level photoemission spectra excited with 130 eV synchrotron radiation at the ASTRID facility at Aarhus, Denmark. These spectra represent measurements with a maximum surface sensitivity.

Figure 1 shows that the clean silicon surface region has a "bulk" Si $2p_{3/2}$ level at 31 eV kinetic energy, corresponding to a binding energy of 99 eV. The foot at ~31.8 eV is the Si $2p_{3/2}$ core level position assigned to the "rest atoms," and the peak at ~30.7 eV is a composite of the Si $2p_{1/2}$ bulk peak and a Si $2p_{3/2}$ core level due to the "ad-atoms" in the notation of the dimer-ad-atom-stacking fault (DAS) model for the 7×7 surface reconstruction.[23] The kinetic energies in these spectra are determined with a very high precision, while the calibration of the monochromator is only accurate to within 1 eV on an absolute scale. Therefore we normally use kinetic energies.

After the first, short exposure included here, (total nitrogen exposure for 5 min at 300 °C), the bulk Si $2p_{3/2}$ and Si
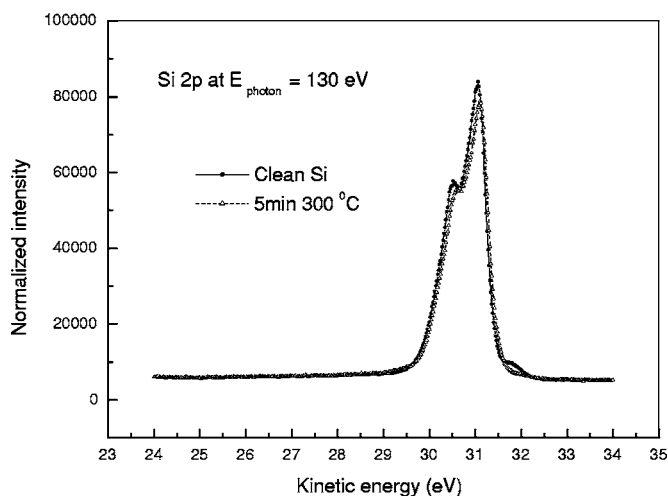

FIG. 1. Si $2p$ spectra at 130 eV photon energy of the Si(111) 7×7 surface. The effect of the first exposure of N (5 min at 2×10^{-7} Torr total nitrogen exposure) is shown at 300 °C.

$2p_{1/2}$ peaks are barely reduced in intensity but the Si $2p_{3/2}$ rest atom peak has disappeared, indicating a change of the surface reconstruction.

The following, larger exposures change the structure of the entire spectrum (see Figs. 2 and 3). The chemically shifted structures toward higher binding energies compared to the bulk peaks (lower kinetic energies) become more dominating. These structures are due to the formation of nitride.

The measurements depicted in Fig. 4 indicate that the nitride growth is self limiting. The final thickness is seen to increase with increasing temperature, as judged from the ratios of nitrided silicon to bulk silicon signals.

All Si $2p$ core-level spectra were systematically analyzed with standard curve-fitting procedures. Using the well known program FitXPS[24] to decompose the Si $2p$ spectra at all steps, in folded, spin-orbit split, Gaussian-Lorentzian peaks, they were seen to consist of the bulk (Si-Si) and up to four components ascribed to various Si-N nearest neighbor configurations.[25]

For fitting the Si $2p$ peaks the following values have been used throughout: Lorentz-full-width-at-half-maximum (LFWHM)=0.18 eV and spin-orbit splitting=0.61 eV. The determination of peak positions was further improved by using identical energy differences between the position of Si^0 and the shifted components Si^{+1}, Si^{+2}, Si^{+3}, and Si^{+4} through all spectral fits. This assures a higher degree of confidence in the results, and in comparisons of relative intensities. Because of the smaller shifts and larger overlaps for this case than for the similar results for oxidation, the uniqueness of the fits might be less convincing in the present case. Thus, we are only discussing tendencies, not the absolute intensities of the peaks.

The principal difference among the spectra in Figs. 2 and 3 is revealed by the decompositions to be due to the intensity changes of the Si^{+2} and the Si^{+3} peaks with temperature. The variable presence of especially Si^{+2} means that the silicon nitride films could be changing structure from amorphous, like the oxide layers,[26] to crystalline.[25] Three other peaks, the
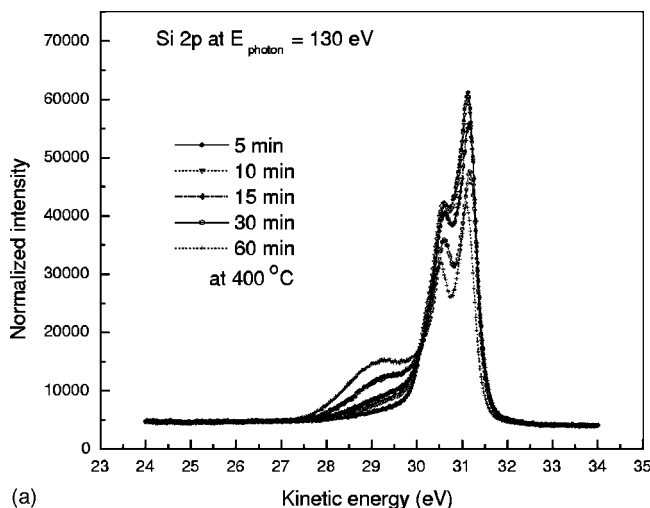
(a)
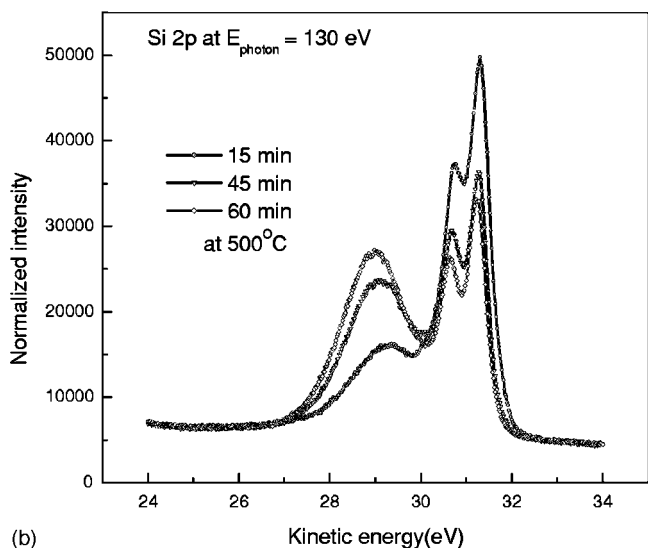
(b)

FIG. 2. Si $2p$ spectra of Si(111) during gradually increasing nitridation [(a): 400 °C and (b): 500 °C].

FIG. 3. Si $2p$ spectra of Si(111) during gradually increasing nitridation at 800 °C.

bulk Si^0, the bulk nitride Si^{+4}, and the Si^{+1} peaks are also changing. The intensity of the bulk Si^0 peaks decrease, while the Si^{+4} peaks increase and the Si^{+1} peaks are changed and move toward lower kinetic energy, with temperature.

In the N 1 s spectra an intense and clearly defined peak is observed at a binding energy of 398.0 eV with a full width at half-maximum of 1.8 eV, at 600 °C. This binding energy is close to the measured value for $Si{\equiv}N$ bonds in Si_3N_4. The other peak, found at 0.7 eV lower kinetic energy, is assigned to $N(-Si)_2$-like bonding as suggested in Ref. 25.

The self-saturating thickness for nitridation increases with increasing temperature (see Fig. 4) like for NH_3 in Ref. 18. The thickness of the nitride layer is determined from N 1 s and from Si $2p$ XPS peak intensities using a common formalism from XPS analysis[3] and plotted in Fig. 8 versus time at 500 °C. The general trend is that the dominant phase in the growing nitride layer for the highest thicknesses and temperatures has Si^{4+} coordination. This kind of growth kinetics is thus similar to the recently discovered behavior of isothermal oxidation processes with pressures of molecular oxygen up to 10^{-87} Torr,[3] except for a very significant dif-
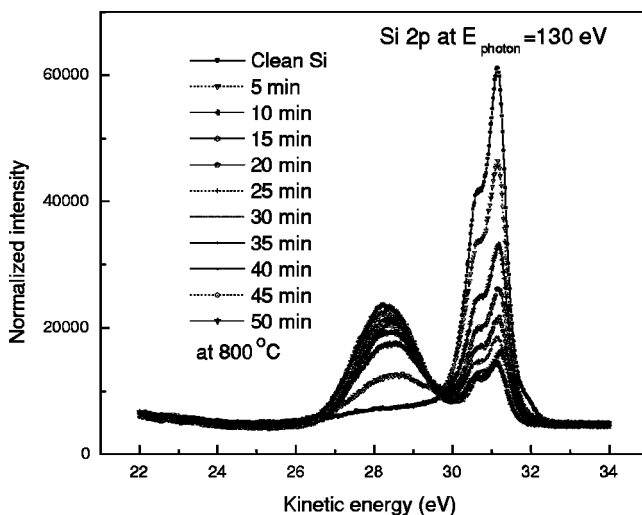
ference: The self-limiting oxide thickness (7–8 Å) is almost independent of the temperature.[3]

The clear trends in Figs. 2 and 3 are that the bulk peaks are reduced in intensity compared to the chemically shifted (nitrided) Si peaks for increasing exposures. The Si^{2+} peaks disappear for $T > 500$ °C and the gap between the bulk peaks becomes deeper due to lowered and shifted Si^{+1} intensities. The nitride features have now become structured but clearly different from a system with silicon-oxygen bonds.

In a parallel set of experiments, using scanning tunneling microscopy (STM), we study the formation of silicon nitride layers (see Fig. 9). These layers were formed and treated at somewhat higher temperatures, and appear as a network of microcrystals.

III. DISCUSSION

The decomposition of the previously discussed spectra, Figs. 5 and 6, and those not shown at 500 °C and 600 °C
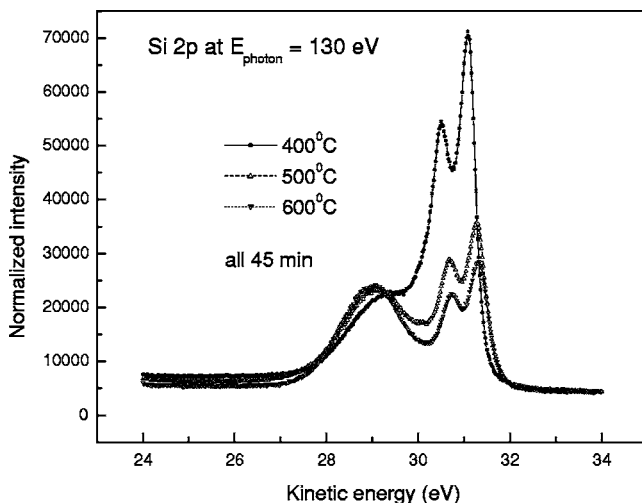

FIG. 4. Comparing the amount of nitride formed at different temperatures.
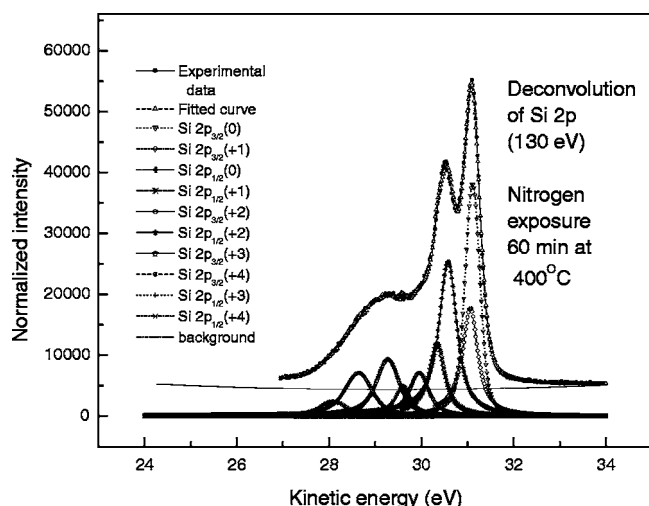
FIG. 5. Decomposition of core-level photoelectron spectra of Si(111) 7×7 exposed at 400 °C.

FIG. 7. N $1s$ spectra at the photon energy 465.5 eV showing two components.

resolves the peaks on the lower kinetic energy side of the bulk Si $2p$ peak ascribable to the Si-N bonding.[25] The shift of the bulk peaks to lower binding energies with nitride on the surface is indicative of an upward band bending indicating that the nitride is negatively charged near the interface.[27–29]

The nitride covers the Si surface uniformly during growth at different temperatures, as seen in Figs. 3 and 8, and is judged to be amorphous for T $\leqslant$ 500 °C from the structure of the interface between the nitride layer and Si, which in these cases contains Si^{1+}, Si^{2+}, and Si^{3+}. Compared to the other cases, and quoting Ref. 25 (see below), a crystalline interface would only contain Si^{1+} and Si^{3+}. Crystallization has further been studied with STM (scanning tunneling microscopy), where a self-limiting nitride film was grown at 800 °C and heated to 1000 °C. Here, the formation of an open network of microcrystallites is seen (also for the grown film). In this situation there are easy conduits for the N atoms (or other
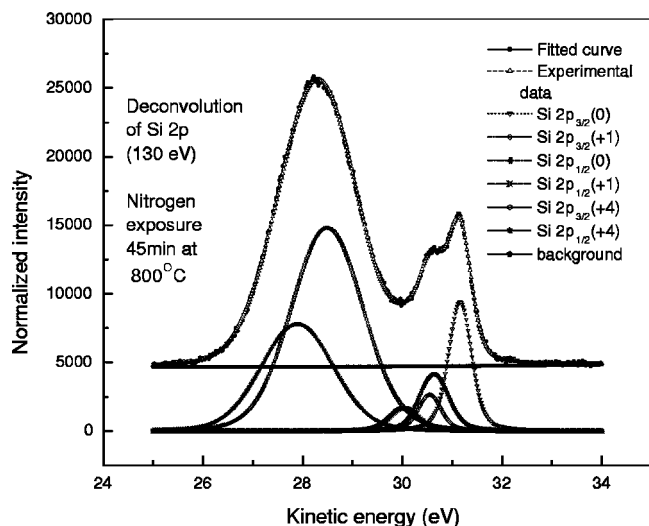
species) to arrive at the bare Si surface and react in the interface region.[30] Thus, these structures do not prevent diffusion.

In the present experiments, one would expect that the amount of Si^{1+} is nearly the same for all samples because it should be located in the interface and therefore should not be sensitive to structural and compositional changes above, inside the nitride film. In the measurements, this would appear in the form of a decreased Si^{1+} intensity as a nitride film grows on top. However, this is not always found here, which might be due to the formation of nonuniform crystallites at higher temperatures.

An important feature of the N 1 s measurements shown in Fig. 7 is that these experiments resolve two components assigned as bulk Si_3N_4 coordinated N and N(-Si_2) bonded N.

From the spectral decompositions demonstrated in Figs. 5 and 6, the Si^{4+} component, assigned to one Si atom bonded to four N atoms, is observed at a binding energy equal to or higher than 2.96 eV with reference to the neutral Si^0 peaks. The tendency of movements toward higher BE for the Si^{4+} component and for thicker films is explained by the electric field across the nitride due to charges in the nitride. The position of the Si^{4+} at the upper part of the film would result in the larger shift for these species in the field. The present results further confirm that thermally grown Si_3N_4 films on Si(111) have a rather abrupt interface, similarly to the crystalline case,[25] at the higher temperatures. The growth at lower temperatures differs, showing a different bonding geometry which we ascribe to the amorphous character of the nitride in these cases. Thus Kim and Yeom[25] showed that the interfacial layer between crystalline Si_3N_4 and Si(111) has no unsaturated bonds, which requires the Si atoms in the interfacial layer to be only in the Si^{1+} or in the Si^{3+} valence states. Hence, as no Si^{2+} species are observed in the Si $2p$ spectra when T $>$ 500 °C in our measurements, this is taken to indicate the same abrupt and defect-free interface as between crystalline β-Si_3N_4 and Si(111).[25]

Kim and Yeom[25] also showed that within a 1×1 surface unit cell, three Si and three N atoms of the topmost layer

FIG. 6. Decomposition of Si $2p$ photoelectron spectra of Si(111) 7×7 exposed to nitrogen for 45 min at 800 °C.
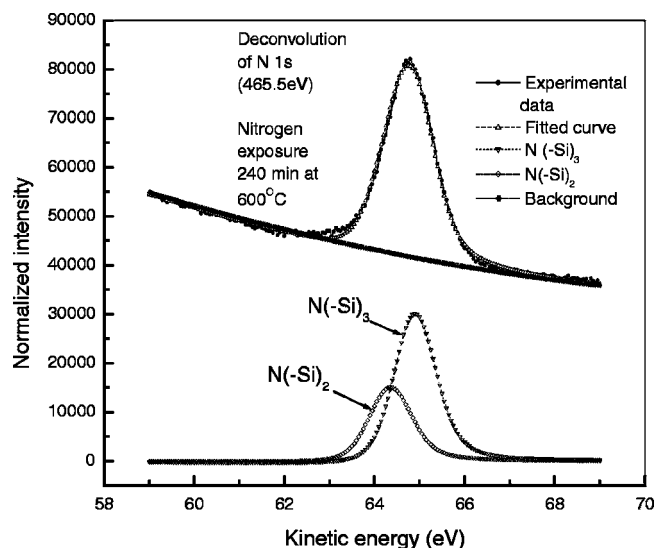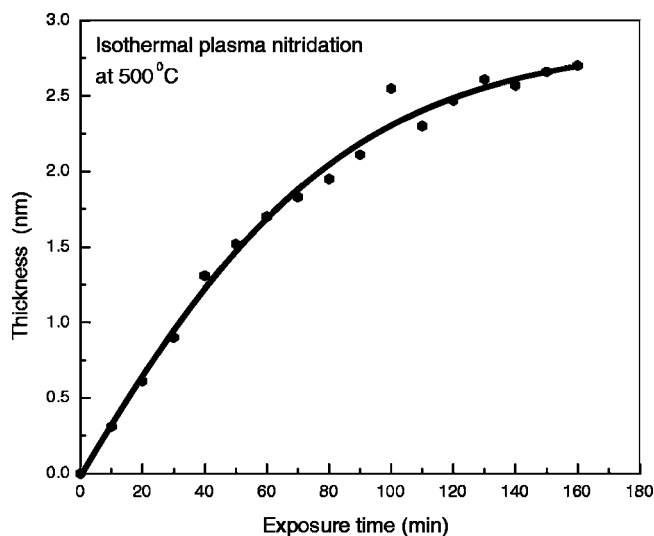
FIG. 8. Isothermal nitridation kinetics of silicon. The nitride thickness vs exposure time at 500 °C.

have a single dangling bond on each Si atom, which should therefore be Si^{3+}. Thus, in this case, three higher-binding energy peaks (Si^{1+}, Si^{3+}, and Si^{4+}) appear with shifts accompanied by a broadening of the bulk component. However, the

shifted N 1s component observed here for the sample grown at 600 °C is most likely due to bulk defects, as the shift of the peak is toward higher binding energies, which might be difficult to assign to surface-bonded N atoms. Furthermore we do not resolve any Si^{3+} component in the Si 2p spectra from the nitride grown at 800 °C. We therefore find no evidence for the particular surface reconstruction reported in Ref. 25, which could be due to a different nature of the present ultrathin films.

IV. CONCLUSIONS

Ultrathin films of pure Si_3N_4 have been grown on Si(111), and different growth steps were studied with various *in situ* spectroscopic techniques such as XPS, STM, and synchrotron radiation-induced high-resolution core level photoemission. The growth of silicon nitride films on Si(111) under these conditions is self limiting, with a final thickness of a few nm, increasing for increasing temperatures.

An N 1s peak at 397.9 eV binding energy is observed during the nitridation of silicon. This peak is attributed to a $N(-Si)_3$ species, like in crystalline silicon nitride, where nitrogen atoms are bonded to three Si atoms in the sp^2 configuration.[18,31] A less intense peak at higher binding energy is assigned to $N(-Si)_2$-like bulk defects.
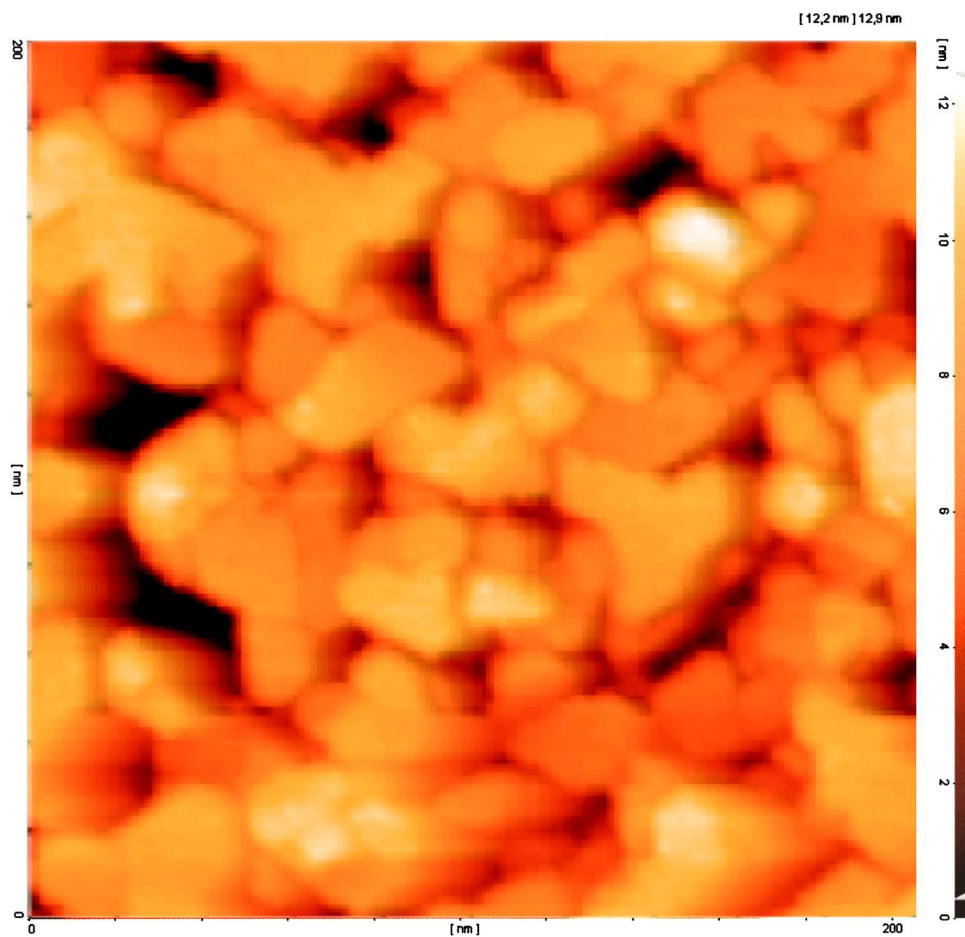

FIG. 9. (Color online) STM of Si_3N_4 crystallites on Si(111) after exposure to nitrogen and heating to 1000 °C. The area covered is 2000 Å by 2000 Å. The height scale covers 0–7 nm.

The Si 2*p* spectra provide the details necessary for monitoring the structure of the nitride and the resulting interface and surface structures. By looking at the relative intensities of the shifted Si 2*p* peaks due to the different Si-N configurations, it is possible to distinguish between amorphous and crystalline structures. Thus the system seems to form with an amorphous nitride structure for growth temperatures lower than 500 °C with a relatively "good" interface. This structure is proposed as a candidate for the gate dielectric for future device applications and should be checked for its electrical characteristics.

[1] P. Morgen, F. K-. Dam, C. Gundlach, T. Jensen, L. B. Tækker, S. Tougaard, and K. Pedersen, Recent Research Developments in Appl. Phys.; Transworld Research Network, **5**, 287 (2002).

[2] D. A. Buchanan and S. H. Lo, Microelectron. Eng. **36**, 13 (1997).

[3] P. Morgen, A. Bahari, U. Robenhagen, J. Andersen, K. Hansen, K. Pedersen, M. G. Rao, and Z. S. Li, J. Vac. Sci. Technol. A **23**(1), 201 (2005).

[4] K. Sekine, Y. Saito, M. Hirayma, and T. Ohmi, IEEE Trans. Electron Devices **47**, 1370 (2000).

[5] S. B. Kang, S. O. Kim, J. S. Byun, and H. J. Kim, Appl. Phys. Lett. **65**, 2448 (1994).

[6] M. Bhat, G. W. Yoon, J. Kim, and D. L. Kwong, Appl. Phys. Lett. **64**, 2116 (1994).

[7] R. Saito, R. Kaluri, and D. W. Hess, Appl. Phys. Lett. **69**, 1053 (1996).

[8] G. Lucovsky, IBM J. Res. Dev. **43**, 301 (1999).

[9] R. I. Hegde, P. J. Tobin, K. Tao, and S. A. Ajuria, Appl. Phys. Lett. **66**, 2882 (1996).

[10] K. A. Ellis and R. A. Buhrman, IBM J. Res. Dev. **43**, 287 (1999).

[11] A. Masuda, I. Fukushi, Y. Yonezawa, A. Morimoto, M. Kumeda, and T. Shimizu, Jpn. J. Appl. Phys., Part 1 **32**, 2794 (1993).

[12] Osamu Jintsugawa, M. Sakuraba, T. Matsuura, and J. Murota, Surf. Interface Anal. **34**, 456 (2002).

[13] G. R. Guusev, H. C. Lu, E. L. Garfunkel, T. Gustafsson, and M. L. Green, IBM J. Res. Dev. **43**, 265 (1999).

[14] E. Cartier, D. A. Buchanan, and G. J. Dunn, Appl. Phys. Lett. **64**, 901 (1994).

[15] P. J. Tobin *et al.*, J. Appl. Phys. **75**, 3548 (1994).

[16] Z. Q. Yao, Appl. Phys. Lett. **64**, 3548 (1994).

[17] Y. Yasuda, S. Zaima, T. Kaida, and Y. Koide, J. Appl. Phys. **67**, 2603 (1990).

[18] X. Shi, M. Shriver, Z. Zhang, T. Higman, and S. A. Campbell, J. Vac. Sci. Technol. A **22**, 1146 (2004).

[19] D. G. J. Sutherland, H. Akatsu, M. Copel, and F. J. Himpsel, J. Appl. Phys. **78**, 6761 (1995).

[20] J. Robertson, J. Vac. Sci. Technol. B **18**, 1785 (2000).

[21] I. Ohshima, W. Cheng, Y. Ono, M. Higuchi, M. Hirayama, A. Teramoto, S. Sugawa, and T. Ohmi, Appl. Surf. Sci. **216**, 246 (2003).

[22] J. H. Stathis, IBM J. Res. Dev. **46**, 265 (2002).

[23] K. Takayanagi, Y. Tanishiro, S. Takahashi, and M. Takahashi, Surf. Sci. **164**, 367 (1985).

[24] D. Adams and J. N. Andersen, FITXPS: A fitting program for core-level spectra available from: http://www.sljus.lu.se/download.html

[25] J. W. Kim and H. W. Yeom, Phys. Rev. B **67**, 035304 (2003).

[26] F. J. Himpsel, F. R. McFeely, A. Taleb-Ibrahimi, J. A. Yarmoff, and G. Hollinger, Phys. Rev. B **38**, 6084 (1988).

[27] S. Nedelec, D. Mathiot, M. Gauneau, and A. Straboni, J. Non-Cryst. Solids **187**, 106 (1995).

[28] H. Hwang, W. Ting, B. Matiti, D. L. Kwong, and J. Lee, Appl. Phys. Lett. **57**, 1010 (1990).

[29] S. Zhixu, S. Tinkler, and D. K. Schroder, IEEE Electron Device Lett. **19**, 237 (1998).

[30] J. Stober, B. Eisenhut, G. Rangelov, and Th. Fauster, Surf. Sci. **321**, 111 (1994).

[31] V. M. Bermudez and F. K. Perkins, Appl. Surf. Sci. **235**, 406 (2004).